Critical Conditions for Binding of Dimethyldodecylamine Oxide Micelles to Polyanions of Variable Charge Density

X. H. Feng,[†] P. L. Dubin,* H. W. Zhang,[‡] G. F. Kirton, P. Bahadur,[§] and J. Parotte

Department of Chemistry, Indiana University−Purdue University at Indianapolis, Indianapolis, Indiana 46202

Received February 20, 2001; Revised Manuscript Received May 18, 2001

ABSTRACT: The binding of *N*,*N*-dimethyldodecylamine oxide micelles to oppositely charged polyanions of variable charge density, namely sulfonated poly(vinyl alcohol) (PVAS) and random copolymers of 2-(acrylamido)-2-methylpropanesulfonate and acrylamide (P(AMPS-AAm)), was studied using turbidimetry, dynamic light scattering, and potentiometric titration. Complexation occurs at a well-defined critical pH corresponding to a critical micelle surface charge density σ_c. The effects of ionic strength I on σ_c and polyelectrolyte average structural charge density $\bar{\xi}$ conform to $\sigma_c\bar{\xi}^a \sim \kappa^b$, where κ is the Debye−Hückel parameter proportional to $I^{1/2}$. Taken along with previous studies, the results show that the exponent b for cylindrical micelles is larger than that for spherical micelles. The effects of $\bar{\xi}$ cannot be explained solely on the basis of average charge spacing but must also take into account the sequence distributions of charged residues.

Introduction

The binding of polyelectrolytes to oppositely charged colloidal particles and surfaces has attracted extensive theoretical investigation[1−6] because of its importance in industrial processes[7−12] and biological systems.[13−19] The results of theoretical treatments[1−4] may be expressed as

$$\sigma_c q \sim \kappa^b \tag{1}$$

where σ_c is the surface charge density of the colloid plane, q is the charge per polymer repeat unit, κ is the Debye−Hückel parameter (for a univalent salt at 25 °C, $\kappa = 3.281 \times I^{1/2}$, where I is in units of mol L^{-1}, κ in nm^{-1}), and the exponent b is reported as 3, 1, and 11/5 in refs 1, 2, and 3, respectively.

Experimentally we have demonstrated the validity of eq 1 for many systems of polyelectrolytes and oppositely charged micelles or dendrimers.[20−25] Examples include the systems comprised of cationic micelles of dimethyldodecylamine oxide (DMDAO) along with polyanions such as sodium poly(styrenesulfonate) (NaPSS) or poly(2-acrylamido-2-methylpropanesulfonate) (PAMPS)[22] or anionic/nonionic mixed micelles along with the polycation poly(dimethyldiallylammonium chloride) (PDMDAAC);[25] the ionic strength dependence of σ_c seems to show validity of eq 1 with $b = 1.0-1.4$. However, these studies were confined to the region of spherical micelles and highly charged polymers. It may be expected that micelle shape, polyelectrolyte charge density, and polyelectrolyte chain flexibility all have effects on the interaction between micelles and polyelectrolytes. For example, Wang et al.[26] studied the interaction of DNA with DMDAO micelles and observed different ionic strength dependences of σ_c for spherical micelles and cylindrical micelles. A single study[23] explored the effect of polyelectrolyte charge density on the binding of linear poly(ethylenimine), LPEI, to mixed micelles of sodium dodecyl sulfate and Triton X-100 by varying the pH. At constant micelle composition (i.e., constant σ), the critical degree of protonation of LPEI, proportional to q in eq 1, was found to be a linear function of the square root of the ionic strength. Wallin and Linse[5,6] used Monte Carlo simulations to study the effects of polyelectrolyte chain flexibility and charge density on complexation with an oppositely charged micelle. Their results showed that increased polyelectrolyte chain stiffness results in decreased binding. Consequently, there is a strong accumulation of polyelectrolyte charges close to the micelle surface for polyelectrolytes with high linear charge density, whereas less charges accumulate close to the micelle surface for polyelectrolytes with lower linear charge density.

In this work, we extend our studies by examining complex formation of micelles of both spherical and cylindrical geometry with structurally similar polyelectrolytes with different linear charge densities. With regard to the micelles, we use DMDAO, a nonionic−cationic surfactant with unique micellar characteristics. First, its micelle surface charge density can be varied precisely through changing the degree of protonation by pH adjustment. Second, it has a clearly defined micelle surface, whereas most nonionic surfactants have very large headgroups so that the corresponding micelle rugosity confounds the concept of a micelle "surface". Third, DMDAO micelles adopt spherical or cylindrical geometry depending on the degree of protonation and on ionic strength.[28,29] Binding studies of DNA to DMDAO micelles[26] show binding behavior in the nonspherical micelle regime that is not dependent on the dimensions of the micelles but is distinctly different from binding to spherical micelles. For this reason, we find it useful to categorize solution conditions according to these two states of micelle shape. From DLS measurements of DMDAO micelles,[29] a criterion of 3 nm for the measured micelle radius is considered to be the limit of the spherical micelle regime.

* To whom correspondence should be sent.
[†] Current address: Department of Chemistry, Hubei University, Wuhan, China.
[‡] Current address: SLTP Co. Ltd., Shanghai, China.
[§] Current address: Department of Chemistry, University of South Gujarat, India.

10.1021/ma010304l CCC: $20.00
Published on Web 07/31/2001

In general, three experimental approaches have been used to systematically vary polymer charge density: (a) pH adjustment of a weak polyacid or polybase,[27,30] (b) derivatization of a nonionic polymer,[31] or (c) copolymerization of nonionic/ionic monomers.[32] However, in method a, charges are mobile ("annealed"): the local charge density of the polyelectrolyte can be affected by the electrostatic field of a charged colloid, which changes the effective pK_a of nearby polymer ionizable residues. In method b, derivatization of some nonionic polymers will yield products of variable hydrophobicity, e.g., as in partial sulfonation of polystyrene.[31] The same problem arises in method c when the nonionic monomer is hydrophobic. In this study, we apply methods b and c, while ensuring that polymer hydrophilicity is not altered. Our first approach was to achieve variations of charge density by sulfation of a hydrophilic polymer, namely poly(vinyl alcohol).[33] Unfortunately, the usefulness of sulfonated poly(vinyl alcohol) (PVAS) as a model polyelectrolyte is compromised by its instability: solutions of PVAS become progressively more acidic on storage; lyophilized highly sulfated samples gradually turn blue and yield insoluble material, both effects increasing with sulfation;[33] and elemental analyses are inconsistent with the degrees of sulfation determined by pH titration of ion-exchanged, fully protonated, samples. All of these observations are consistent with hydrolysis and cyclization of PVAS to form intramolecular or intermolecular sulfone linkages. In view of the difficulties that might be anticipated in repeating such studies elsewhere with PVAS, we also studied a second class of polyions of similarly variable charge density, namely AMPS−acrylamide copolymers. This also provides the opportunity to observe the effect of segment sequence distributions, which are expected to differ for the two types of polyions.

Experimental Section

Materials. *N*,*N*-Dimethyldodecylamine oxide (DMDAO) was from Sigma (St. Louis, MO), purity >97%. Poly(vinyl alcohol sulfate) sodium salts (PVAS) were prepared by sulfation of poly(vinyl alcohol) (Aldrich, MW = 13 000−23 000), followed by neutralization by NaOH.[33] Degrees of sulfation were determined from elemental analysis as 25.3%, 57.5%, and 80.1% for the three PVAS samples used in this work. Random copolymers of 2-(acrylamido)-2-methylpropanesulfonate (AMPS) and acrylamide (AAm) with AMPS mole fractions ranging from 10% to 100% were synthesized in DMF and purified using the procedures described in ref 34. Their molecular weights as estimated from apparent hydrodynamic radii (see below) were ca. 2×10^5. The linear average polymer charge density $\bar{\xi}$ (we will comment below in more detail about the importance of recognizing $\bar{\xi}$ as an average quantity) was calculated from $\bar{\xi} = e^2/4\pi\epsilon_0\epsilon_r kTl$, where e is the elementary charge (C), ϵ_0 and ϵ_r are respectively the permittivity of a vacuum (C V^{-1} m^{-1}) and the solvent dielectric constant, k is the Boltzmann constant, T is the absolute temperature, and l is the average charge spacing along the polymer chain (m). The linear charge density of vinyl polymers with a charge spacing of 2.55 Å is $\bar{\xi}$ = 2.80. The values of $\bar{\xi}$ for PVAS and copolymers were obtained by multiplying 2.80 by the degrees of sulfation and the mole fraction of AMPS, respectively. All values of $\bar{\xi}$ are listed in Table 1. Water from a Milli-Q purification system was used throughout the work.

Potentiometric Titration. The relationship between pH and the degree of protonation β of DMDAO micelles was obtained by pH titration of 10 or 50 mM DMDAO using a Beckman ϕ34 pH meter equipped with a Beckman combination electrode, at 25 ± 1 °C, under N_2 and magnetic stirring, using procedures described elsewhere.[20,29]

Table 1. Average Linear Charge Densities for Polymers Used in This Study

PVAS	$\bar{\xi}$	copolymers	$\bar{\xi}$
25.3% sulfated	0.71	10% AMPS	0.28
57.5% sulfated	1.61	25% AMPS	0.70
80.1% sulfated	2.24	50% AMPS	1.40
		100% AMPS	2.80

Turbidimetric Titration. Turbidimetric titrations were carried out at 25 ± 1 °C by adding 0.100−0.500 M HCl to mixed solutions of 10 mM DMDAO and 0.5 g L^{-1} PVAS or 50 mM DMDAO and 0.1 g L^{-1} copolymer at fixed ionic strengths I, monitoring pH and turbidity simultaneously. Turbidity measurements, reported as 100 − %T, were carried out at 420 nm using a Brinkmann PC 800 probe colorimeter equipped with a 1 cm path length fiber optics probe. The measured turbidity values were corrected by subtracting the turbidity of a polymer-free blank. The pH and turbidity values were recorded after the values became stable (about 2 min).

Dynamic Light Scattering (DLS). Solutions of 50 mM DMDAO at various ionic strengths and pH were introduced into 7 μL cells through 0.20 μm filters. Measurements were carried out at 90° scattering angle and at 25 ± 1 °C with a DynaPro-801 system (Protein Solutions Inc., Charlottesville, VA) equipped with a 30 mW solid-state 780 nm laser and an avalanche photodiode detector. The correlation function of the scattered light intensity was analyzed by the program CONTIN[35] to obtain the diffusion coefficient, D, of the micelles. This coefficient was converted to the apparent hydrodynamic radius, R_h, of the micelle using the Stokes−Einstein equation for a sphere

$$R_h = kT/6\pi\eta D \qquad (2)$$

where k is the Boltzmann constant, T is the absolute temperature, and η is the solvent viscosity.

Results

Turbidimetric titrations were performed for systems of DMDAO and three kinds of PVAS of different linear charge densities. As a representative set of plots, Figure 1 shows the change of turbidity, expressed as 100 − %T, with pH for 80.1% sulfated PVAS at various ionic strengths. The point of initial increase in turbidity is designated as pH_c, corresponding to the initial formation of the polymer−DMDAO complex. As seen from Figure 1, pH_c, which corresponds to the degree of micelle protonation at incipient binding, β_c, decreases with increasing ionic strength. The increase in β_c upon addition of salt is due to the attenuation of interaction by increased electrostatic shielding.

Plots of the turbidity vs pH for the four copolymers at different ionic strengths are shown in Figure 2. The

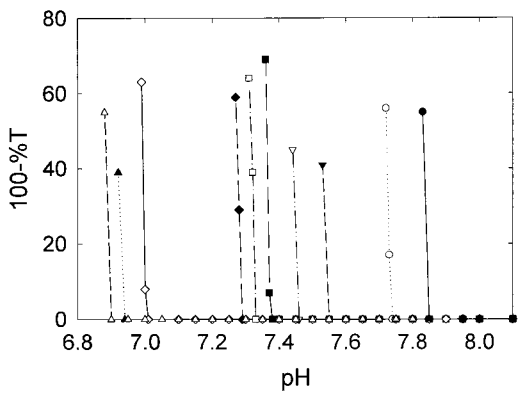

Figure 1. Turbidimetric titration of 0.5 g L^{-1} PVAS (80.1% sulfated) and 10 mM DMDAO at I = 1.00, 0.80, 0.60, 0.40, 0.25, 0.20, 0.15, 0.10, 0.06, and 0.04 (from left to right).

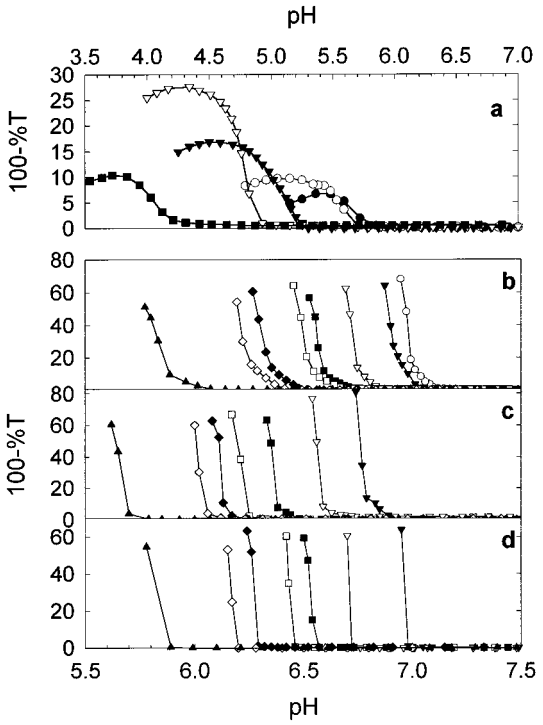

Figure 2. Turbidimetric titration of 0.1 g L^{-1} P(AMPS−AAm) and 50 mM DMDAO at $I = 0.015$ (●), 0.05 (○), 0.1 (▼), 0.2 (▽), 0.3 (■), 0.4 (□), 0.5 (◆), 0.6 (◇), and 0.9 (▲): (a) 10% AMPS; (b) 25% AMPS; (c) 50% AMPS; (d) 100% AMPS.

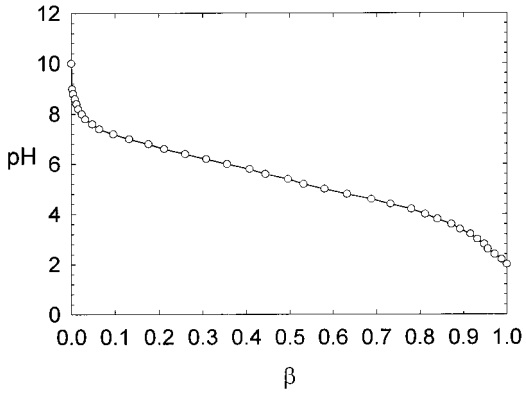

Figure 3. pH titration curve of 50 mM DMDAO, expressed as pH vs β at $I = 0.80$.

effects of ionic strength are seen to be similar to those found for PVAS. An important observation, however, is that the curves for the copolymer with 10% anionic content are clearly less abrupt than the other copolymers in Figure 2. This feature will be discussed at length below.

The pH_c values for all DMDAO−polymer systems may be converted to critical values of the degree of ionization, β_c, using plots of pH vs β at the 15 different ionic strengths employed in this study; a representative plot for $I = 0.8$ is shown in Figure 3. The resulting β_c values for the seven different polymers at different ionic strengths are shown in Tables 2 and 3. The dependence of β_c on ionic strength is presented for all systems in Figure 4, in which filled and open symbols correspond to cylindrical ($R_h > 3$ nm) or spherical micelles, respectively. To analyze our results in terms of eq 1, we converted β_c to the critical micelle surface charge density σ_c by using the following procedures. First, the micelle surface potential ψ_o(V) at β_c was calculated from[36]

Table 2. Electrostatic Properties of DMDAO Micelles at pH and Ionic Strengths Corresponding to Critical Conditions for Binding of AMPS−AAm Copolymers

I	κ (Å^{-1})	pK_0	pH_c	β_c	pK_β	ψ_0 (mV)	R_h (Å)	$\sigma_c \times 10^2$ (C m^{-2})
			P(AMPS10/AAm90)−DMDAO					
0.015	0.040	5.91	5.90	0.18	5.22	40.9	18	2.73
0.05	0.073	6.03	5.71	0.24	5.32	42.0	23	3.39
0.10	0.104	6.10	5.30	0.31	5.31	46.8	44	4.34
0.20	0.147	6.17	4.95	0.52	5.02	68.1	93	9.85
0.30	0.180	6.24	4.25	0.69	4.69	91.8	107	19.5
			P(AMPS25/AAm75)−DMDAO					
0.05	0.073	6.03	6.88	0.06	5.82	12.4	24	1.00
0.10	0.104	6.10	6.78	0.10	5.85	14.8	25	1.49
0.20	0.147	6.17	6.54	0.16	5.82	20.7	30	2.60
0.30	0.180	6.24	6.33	0.21	5.81	25.5	51	3.60
0.40	0.208	6.31	6.27	0.25	5.85	27.2	69	4.42
0.50	0.232	6.33	5.98	0.33	5.73	35.5	121	6.58
0.60	0.254	6.37	5.85	0.37	5.70	39.7	158	8.15
0.90	0.311	6.41	5.34	0.52	5.40	59.8	277	16.7
			P(AMPS50/AAm50)−DMDAO					
0.10	0.104	6.10	6.91	0.08	5.90	11.8	24	1.19
0.20	0.147	6.17	6.70	0.13	5.88	17.2	27	2.19
0.30	0.180	6.24	6.48	0.18	5.88	21.3	41	2.98
0.40	0.208	6.31	6.34	0.24	5.86	26.6	62	4.32
0.50	0.232	6.33	6.24	0.29	5.82	30.2	86	5.48
0.60	0.254	6.37	6.12	0.31	5.84	31.4	117	6.23
0.90	0.311	6.41	5.79	0.41	5.71	41.4	225	10.4
			PAMPS−DMDAO					
0.10	0.104	6.10	6.98	0.07	5.93	10.1	24	1.02
0.20	0.147	6.17	6.72	0.12	5.90	16.0	27	2.04
0.30	0.180	6.24	6.57	0.17	5.90	20.1	36	2.80
0.40	0.208	6.31	6.46	0.22	5.89	24.9	53	4.01
0.50	0.232	6.33	6.29	0.28	5.83	29.6	82	5.36
0.60	0.254	6.37	6.20	0.30	5.85	30.8	109	6.10
0.90	0.311	6.41	5.89	0.38	5.78	37.3	205	9.20

$$pK_0 - pK_\beta = 0.434\psi_0 e/kT \tag{3}$$

where pK_0 is the intrinsic logarithmic ionization constant (pK_β at $\beta = 0$) and e is the elementary charge (C). For spherical micelles, σ (C) at β_c may then be calculated by the Gouy−Chapman equation for spherical particles[37]

$$\sigma = \epsilon_0\epsilon_r\psi_0/(1/r + \kappa) \tag{4}$$

where ϵ_0 and ϵ_r are respectively the vacuum permittivity (C V^{-1} m^{-1}) and the dimensionless dielectric constant of solvent, r is the micelle radius (m) at β_c, and κ is the Debye−Hückel parameter (m^{-1}). For micelles with cylindrical geometry, i.e., $R_h > 3$ nm, σ is calculated from[38]

$$\sigma = \epsilon_r\epsilon_0\kappa kTP/e \tag{5}$$

with

$$P = 2\sinh(y/2)[1 + (B^{-2} - 1)/\cosh^2(y/4)]^{1/2} \tag{6}$$

where

$$y = e\psi_0/kT \tag{7}$$

$$B = K_0(A)/K_1(A) \tag{8}$$

$$A = \kappa r \tag{9}$$

and where r is the minor axis radius of the cylinder, which is assumed to be equal to the radius of the largest spherical micelle (3 nm), $K_0(A)$ is the zero-order modified Bessel function of the second kind,[39] and $K_1(A)$ is the

Table 3. Electrostatic Properties of DMDAO Micelles at pH and Ionic Strengths Corresponding to Critical Conditions for Binding of PVAS[a]

I	κ (Å^{-1})	pK_0	pH$_c$	β_c	pK_β	ψ_0 (mV)	$\sigma_c \times 10^3$ (C m^{-2})
			PVAS, 25.3% Sulfated				
0.04	0.066	6.04	6.90	0.07	5.79	14.7	10.8
0.06	0.082	6.05	6.79	0.09	5.78	15.6	13.2
0.10	0.104	6.10	6.73	0.10	5.78	18.6	18.6
0.15	0.127	6.14	6.65	0.13	5.82	18.8	21.9
0.20	0.147	6.17	6.63	0.14	5.84	19.2	24.9
0.25	0.164	6.21	6.64	0.15	5.90	18.3	25.9
0.40	0.208	6.30	6.55	0.19	5.93	21.6	37.1
0.60	0.254	6.37	6.44	0.22	5.90	27.7	56.6
0.80	0.293	6.40	6.23	0.31	5.89	29.9	69.2
1.00	0.328	6.42	6.10	0.35	5.83	35.2	90.0
			PVAS, 57.5% Sulfated				
0.04	0.066	6.04	7.28	0.04	5.91	8.4	6.19
0.06	0.082	6.05	7.13	0.05	5.86	12.4	10.5
0.10	0.104	6.10	7.07	0.06	5.88	12.8	12.8
0.15	0.127	6.14	7.07	0.07	5.95	11.0	12.8
0.20	0.147	6.17	7.01	0.08	5.95	12.7	16.5
0.25	0.164	6.21	6.98	0.09	5.99	13.2	18.8
0.40	0.208	6.30	6.89	0.13	6.05	14.6	25.1
0.60	0.254	6.37	6.74	0.17	6.05	18.7	38.3
0.80	0.293	6.40	6.68	0.20	6.07	19.0	44.0
1.00	0.328	6.42	6.55	0.24	6.06	21.5	55.1
			PVAS, 80.1% Sulfated				
0.04	0.066	6.04	7.85	0.01	5.93	7.05	4.53
0.06	0.082	6.05	7.74	0.02	5.95	7.01	5.15
0.10	0.104	6.10	7.55	0.03	5.98	7.29	6.18
0.15	0.127	6.14	7.46	0.04	6.03	6.36	6.26
0.20	0.147	6.17	7.38	0.05	6.05	6.89	7.54
0.25	0.164	6.21	7.33	0.05	6.09	7.28	10.3
0.40	0.208	6.30	7.29	0.07	6.16	8.26	14.2
0.60	0.254	6.37	7.01	0.12	6.12	14.6	29.9
0.80	0.293	6.40	6.94	0.14	6.15	14.3	33.0
1.00	0.328	6.42	6.90	0.16	6.18	14.2	36.1

[a] Micelles in the spherical region were assumed to have a radius of 2.5 nm; micelles in the cylindrical region were assumed to have a minor axis radius of 3 nm (the largest observed sphere radius, see Table 2).

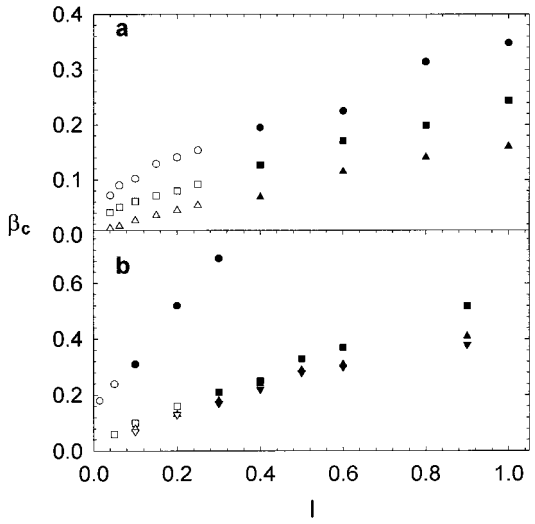

Figure 4. Dependence of the critical degree of protonation of DMDAO micelles on ionic strength for PVAS−DMDAO and P(AMPS−AAm)−DMDAO systems. Open and filled symbols represent spherical and cylindrical micelle regions, respectively. (a) PVAS with degree of sulfation 25.3% (○ and ●), 57.5% (□ and ■), and 80.1% (△ and ▲). (b) P(AMPS−AAm) with 10% AMPS (○ and ●), 25% AMPS (□ and ■), 50% AMPS (△ and ▲), and 100% AMPS (▽ and ▼).

first-order modified Bessel function of the second kind.[39] Resulting values of σ_c obtained over a wide range of

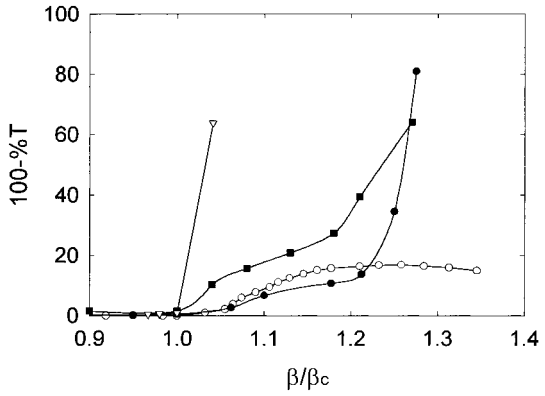

Figure 5. Dependence of turbidity on β/β_c for P(AMPS−AAm)−DMDAO systems at $I = 0.10$: (○) 10% AMPS; (■) 25% AMPS; (●) 50% AMPS; (▽) 100% AMPS.

polymer types and ionic strengths are summarized in Tables 2 and 3.

Discussion

As seen in Figure 2a, the maximum turbidity of the copolymer with 10% AMPS is low compared to that of the other copolymers. This suggests that complexes formed in this system are weak scatterers; i.e., the complex species formed are different from those for other copolymers. In fact, no phase separation is observed for 10% AMPS, and the maximum in turbidity corresponds to the formation of soluble complexes, followed by their redissolution at low pH due to charge reversal. Figure 2 also shows that the abruptness of the increase in turbidity decreases with decreasing AMPS content. Comparison among the copolymers is more clearly shown by plots of turbidity vs β/β_c given for $I = 0.1$ in Figure 5. The more gradual changes for lower ξ copolymers could indicate that micelle binding increases gradually with β for those, but abruptly for PAMPS. We recently found[40] that the binding constant for complexation of DMDAO micelles with NaPSS at $I = 0.2$ is negligible at $\beta < 0.1$ but increases quite dramatically between $\beta = 0.11$ and $\beta = 0.13$. Since PAMPS and NaPSS have similar charge densities, a similar tendency is expected for PAMPS.

To compare our results with eq 1, the ionic strength dependence of the surface charge densities at critical conditions is presented in Figure 6 as log σ_c vs log κ for both types of polyelectrolytes, where open and filled symbols represent spherical and cylindrical micelles, respectively. By linear fitting of log−log plots in the regimes of spherical and cylindrical micelles, we obtained slopes (corresponding to b in eq 1) of 1.0 ± 0.2 for PVAS and 1.4 ± 0.2 for copolymers in the spherical micelle region and 1.8 ± 0.2 for PVAS and 2.5 ± 0.3 for copolymers in the cylindrical micelle region. Thus, we can observe that for both types of polyelectrolytes the value of b for cylindrical micelles is larger than that for spherical micelles. We previously observed $b = 1.4$ in the spherical micelle region for DMDAO with both NaPSS and P(AMPS−NVP) (64:36).[25] In a more recent study on the interaction of DNA with DMDAO micelles,[26] the slopes of log β vs log I were found to be 0.8 and 0.9 for spherical and cylindrical micelles, corresponding respectively to $b = 1.6$ and $b = 1.8$. This again shows a larger value for the more elongated micelles (although the difference was small in the case of this rodlike polyelectrolyte). But for flexible polyanions we

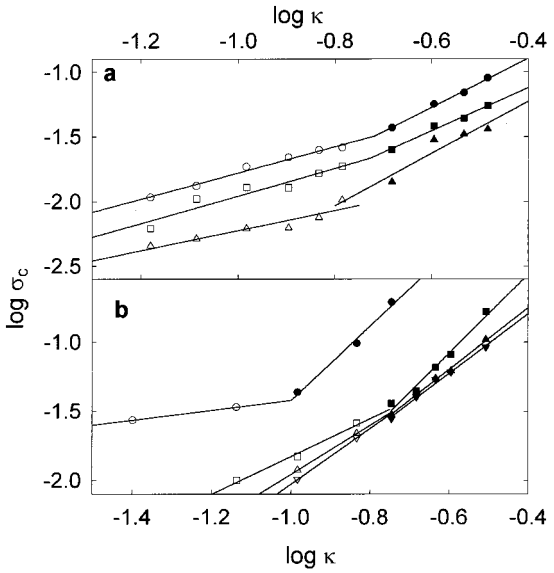

Figure 6. log σ_c−log κ plots for (a) PVAS−DMDAO systems and (b) P(AMPS−AAm)−DMDAO systems. Symbols are the same as in Figure 4.

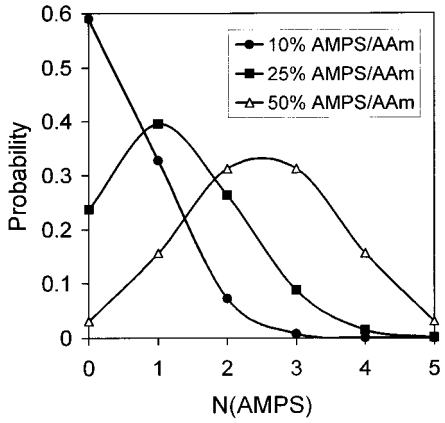

Figure 7. Distribution of pentad compositions based on the conditions of AMPS/AAm copolymerization for the given copolymer samples.

can summarize our results as follows: for spherical DMDAO micelles, *b* is around 1.4, whereas for cylindrical DMDAO micelles, *b* is around 2.0. It may be worth noting that the theoretical values of *b* for polyelectrolyte adsorption on planes of 11/5 (ref 3) and 3 (ref 1) are closer to our experimental values for cylindrical micelles than to our results for spherical micelles. On the basis of these observations, we may speculate that $b_{\text{sphere}} < b_{\text{cylinder}} < b_{\text{plane}}$. This relationship may represent the effect of micelle geometry on the interaction between polyelectrolytes and oppositely charged colloids.

While theoretical treatments describe the polymer charge via "*q*", the charge per repeat unit, the relationship between this variable and the charge structural parameter of any real polyelectrolyte must be considered, since reduction in "polymer charge density" in the real case corresponds to an increase in the mean distance between charged residues, not a decrease in charge per residue. More importantly, nonuniform spacing between charged residues will be the rule, not the exception. Such effects can be seen in Figures 4 and 6. As displayed in Figures 4 and 6, the relative effect of $\bar{\xi}$ on β_c is substantially larger for PVAS than for copolymers in the range $0.70 < \bar{\xi} < 2.80$; i.e., PVAS samples with $\bar{\xi} = 1.61$ and 2.24 display different σ_c values, while copolymers with $\bar{\xi} = 1.40$ and 2.80 are nearly indistinguishable with respect to σ_c. We believe that this effect is due to different types of segment sequence distributions for the two types of polymers.

Sequence distributions can be calculated from reactivity ratios and monomer feed compositions.[41] The reactivity ratios for AMPS and AAm copolymerizing in DMF are reported[42] to be $r_1 = 1.00 \pm 0.03$ and $r_2 = 1.02 \pm 0.10$. Therefore, the copolymers used in this study have essentially a random segment sequence distribution. Previous work[25,31b] suggests that incipient binding of polyelectrolytes to DMDAO micelles is sensitive to cooperatively bound sequences of five charged residues. The pentad sequence distributions for AMPS/AAm copolymers were therefore calculated and are shown in Figure 7. The probability of finding pentads that are fully AMPS is 0.03 for 50% AMPS copolymer, 0.001 for 25% AMPS copolymer, and less than 10^{-5} for 10% AMPS copolymer. The similar values of σ_c observed for 50% AMPS copolymer and PAMPS (see Figure 6) could be best explained by assuming that incipient binding is determined by the most highly charged pentads, whose presence above the threshold concentration of 3% determines an effective $\xi > \bar{\xi}$ and hence a corresponding σ_c. Pentads containing four AMPS must also bind, because σ_c can be observed for the 25% AMPS copolymer that is seen to have negligible amounts of AMPS pentads. The probabilities of such 80% sulfonated pentad sequences are 0.16 for 50% AMPS, 0.015 for 25% AMPS, and less than 0.0005 for 10% AMPS. The very low probability of highly charged sequences for 10% AMPS copolymer would explain its different binding behavior seen in Figure 6b compared to the other AMPS/AAm copolymers. In contrast, Figure 6a for PVAS shows a more uniform effect of $\bar{\xi}$ on σ_c. The sulfation of PVA involves the ionization of a hydroxyl group in the vicinity of an already sulfonated residue, so the formation of adjacent sulfonated sites is unfavorable, and PVAS has a more regular segment sequence distribution. Therefore, polymers with different $\bar{\xi}$ values exhibit correspondingly different values of σ_c.

We now turn our attention to the relationship between ionic strength, critical micelle surface charge density σ_c, and polyelectrolyte charge density. Using the values of *b* obtained from Figure 6, we found that plots of $(\sigma_c\bar{\xi})$ vs κ^b (see eq 1) for the seven polymers all diverged, even within a given group. Recognizing that the relationship between *q* in eq 1 and $\bar{\xi}$ is unknown, for the reasons given above, we attempted to fit the data to a modified form of eq 1, namely $\sigma_c\bar{\xi}^a \sim \kappa^b$, where *a* is an empirical fitting parameter. The results are shown in Figure 8, with $a = 0.6$ for PVAS and $a = 0.2$ for AMPS/AAm copolymers, except for the 10% AMPS copolymer. Although *a* and *b* are adjustable parameters, the fitting over a wide range of ionic strengths and polymer compositions are of good quality, and the straight lines extrapolate to $\sigma_c = 0$ at $\kappa = 0$ as expected from eq 1.

The anomalous behavior of the data for 10% AMPS copolymer in Figure 6b can now be explained by the difference between effective ξ (ξ_{eff}) and $\bar{\xi}$. For PVAS, the uniform spacing of charged sulfonate groups leads to $\xi_{\text{eff}}/\bar{\xi}$ close to 1. $\bar{\xi}$ thus has a larger effect on σ_c for PVAS than for the AMPS/AAm copolymers. Indeed, Dubin et al.[27] found for partially protonated LPEI that $a \approx 1$ for constant micelle surface charge density, indicating that $\xi_{\text{eff}}/\bar{\xi} \approx 1$. The random composition of AMPS/AAm

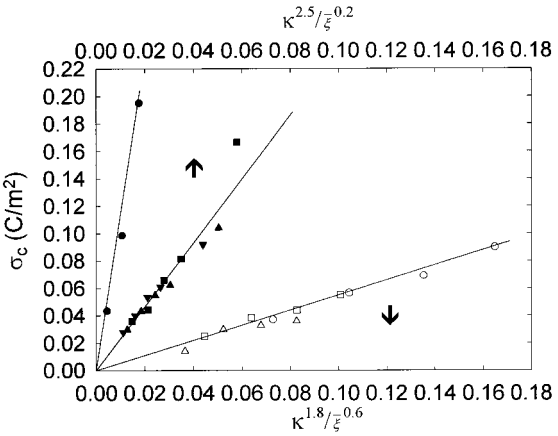

Figure 8. Dependence of critical micelle surface charge density on $\kappa^{1.8}/\bar{\xi}^{0.6}$ for PVAS and on $\kappa^{2.5}/\bar{\xi}^{0.2}$ for copolymers in the region of cylindrical micelles. Open and filled symbols represent PVAS and copolymers, respectively. (○) 25.3% sulfated, (□) 57.5% sulfated, (△) 80.1% sulfated, (●) 10% AMPS, (■) 25% AMPS, (▲) 50% AMPS, (▼) 100% AMPS.

copolymers leads through the presence of highly sulfonated pentads to $\xi_{eff} > \bar{\xi}$. This leads to a weaker effect of a reduction in $\bar{\xi}$ and thus to the smaller value of a observed in Figure 8 relative to PVAS. As the probability of finding AMPS pentads decreases, the ratio $\xi_{eff}/\bar{\xi}$ increases. The effect would be far more dramatic for the 10% AMPS copolymer, as determined from the probabilities in Figure 7.

The related low probability of highly charged pentads and high values of β_c for the 10% AMPS copolymer also explains its anomalous behavior in Figure 2a. The charged binding sites in this copolymer are isolated and small in number, whereas the micelles have relatively large charges. Overall charge neutrality for the complex is thus achieved upon binding of a very small number of micelles. Additional binding of micelles may then result in charge reversal and resolubilization for the complex. The results of simulations that reveal loose binding of ionic groups for polymers of low charge density[6] are also consistent with more reversibly soluble complexes as suggested by the results of Figure 2a.

In addition to effective linear charge density, the chain stiffness of the polyelectrolytes is also a factor[5,6] in the binding behavior to DMDAO micelles. For a given $\bar{\xi}$, it is expected that binding would be more difficult for polymers with larger intrinsic persistence lengths. Although measurements of persistence lengths are not available for PVAS and the copolymers, a remarkably large Mark−Houwink−Sakurada parameter ($a \approx 1.0$) was noted[43] for PVAS in 0.5 M NaCl, indicative of a large intrinsic persistence length for PVAS. Binding of PVAS to DMDAO micelles would then be expected to be more difficult than for the P(AMPS/AAm) copolymers. However, as illustrated in Figure 8, PVAS polymers exhibit lower σ_c than P(AMPS/AAm) copolymers of equal $\bar{\xi}$. Polymer stiffness is thus not a dominant factor in the incipient binding to DMDAO micelles.

Conclusions

Incipient complex formation between DMDAO micelles and polyanions of variable charge density $\bar{\xi}$ over a range of ionic strengths can be described by the semiempirical relationship $\sigma_c\bar{\xi}^a \sim \kappa^b$. Both micelle geometry and polymer segment sequence distributions affect this relationship. For flexible polyanions, b is found to be equal to 1.4 and 2.0 for spherical and cylindrical DMDAO micelles, respectively. For a random copolymer, the effective ξ is larger than $\bar{\xi}$, whereas ξ_{eff} is closer to $\bar{\xi}$ for a polymer with a more uniform charge distribution.

Acknowledgment. This work was supported by NSF DMR 0076068. X. H. Feng thanks the China Scholarship Council for a Visiting Research Fellowship for the period of 2000−2001. We thank Prof. Y. Morishima for providing the acrylamide-AMPS copolymers.

References and Notes

(1) Wiegel, F. W. *J. Phys. A: Math. Gen.* **1977**, *10*, 299.
(2) Evers, O. A.; Fleer, G. J.; Scheutjens, J. M. H. M.; Lyklema, J. *J. Colloid Interface Sci.* **1986**, *111*, 446.
(3) Muthukumar, M. *J. Chem. Phys.* **1987**, *86*, 7230.
(4) Odijk, T. *Macromolecules* **1980**, *13*, 1542.
(5) Wallin, T.; Linse, P. *Langmuir* **1996**, *12*, 305.
(6) Wallin, T.; Linse, P. *J. Phys. Chem.* **1996**, *100*, 17873.
(7) Linse, P.; Piculell, L.; Hansson, P. In *Polymer-Surfactant Systems*; Kwak, J. C. T., Ed.; Marcel Dekker: New York, 1998; Chapter 5.
(8) Schwoyer, W. L. K., Ed. *Polyelectrolytes for Water and Wastewater Treatment*; CRC Press: Boca Raton, FL, 1981.
(9) Wagberg, L.; Winter, L.; Ödberg, L.; Lindström, T. *Colloids Surf.* **1987**, *27*, 163.
(10) Read, A. D. *Br. Polym. J.* **1972**, *4*, 253.
(11) Kawabata, N.; Hayashi, T.; Nishikawa, M. *Bull. Chem. Soc. Jpn.* **1986**, *59*, 2861.
(12) Farinato, R. S.; Dubin, P. L. *Colloid-Polymer Interactions: from Fundamentals to Practice*; Wiley-Interscience: New York, 1999.
(13) Margolin, A.; Sherstyuk, S. F.; Izumrudov, V. A.; Zezin, A. B.; Kabanov, V. A. *Eur. J. Biochem.* **1985**, *146*, 625.
(14) Clark, K. M.; Glatz, C. E. *Biotechnol. Prog.* **1987**, *3*, 241.
(15) Fisher, R. R.; Glatz, C. E. *Biotechnol. Bioeng.* **1988**, *32*, 777.
(16) Bozzano, A. G.; Andrea, G.; Glatz, C. E. *J. Membr. Sci.* **1991**, *55*, 181.
(17) Dubin, P. L.; Strege, M. A.; West, J. In *Large Scale Protein Purification*; Ladish, M., Ed.; American Chemical Society: Washington, DC, 1990; Chapter 5.
(18) Shaner, S. L.; Melancon, P. Lee, K. S.; Burgess, M. T.; Record, M. T., Jr. *Cold Spring Harbor Symp. Quantum Biol.* **1983**, *47*, 463.
(19) Von Hippel, P. H.; Bear, D. G.; Morgan, W D.; McSwiggen, J. A. *Annu. Rev. Biochem.* **1986**, *53*, 389.
(20) Dubin, P. L.; Chew, C. H.; Gan, L. M. *J. Colloid Interface Sci.* **1989**, *128*, 566.
(21) Dubin, P. L.; Thé, S. S.; McQuigg, D. W.; Chew, C. H. Gan, L. M. *Langmuir* **1989**, *5*, 89.
(22) McQuigg, D. W.; Kaplan, J. I.; Dubin, P. L. *J. Phys. Chem.* **1992**, *96*, 1973.
(23) Zhang, H.; Dubin, P. L.; Ray, J.; Manning, G. S.; Moorefield, C. N.; Newkome, G. R. *J. Phys. Chem. B* **1999**, *103*, 2347.
(24) Miura, N.; Dubin, P. L.; Moorefield, C. N.; Newkome, G. R. *Langmuir* **1999**, *15*, 4245.
(25) Zhang, H.; Ohbu, K.; Dubin, P. L. *Langmuir* **2000**, *16*, 9082.
(26) Wang, Y.; Dubin, P. L.; Zhang, H. *Langmuir* **2001**, *17*, 1670.
(27) Dubin, P. L.; Curran, M. E.; Hua, J. *Langmuir* **1990**, *6*, 707.
(28) Ikeda, S.; Tsunoda, M.; Maeda, H. *J. Colloid Interface Sci.* **1979**, *70*, 448.
(29) Zhang, H.; Dubin, P. L.; Kaplan, J. I. *Langmuir* **1991**, *7*, 2103.
(30) Hansson, P.; Almgren, M. *J. Phys. Chem.* **1996**, *100*, 9038.
(31) (a) Essafi, W.; Lafuma, F.; Williams, C. E. *J. Phys. II* **1995**, *5*, 1269. (b) McQuigg, D. W. M.S. Thesis, Purdue University, 1991.
(32) (a) Ranganathan, S.; Kwak, J. C. T. *Langmuir* **1996**, *12*, 1381. (b) Hoagland, D. A.; Smisek, D. L.; Chen, D. Y. *Electrophoresis* **1996**, *17*, 1151.
(33) Takahashi, A.; Nagasawa, M.; Kagawa, I. *Kogyo Kagaku Zasshi* **1958**, *61*, 1614.
(34) Morishima, Y.; Ohgi, H.; Kamachi, M. *Macromolecules* **1993**, *26*, 4293.
(35) Provencher, S. W. *Comput. Phys. Commun.* **1982**, *27*, 229.9.
(36) Tokiwa, F.; Ohki, K. *J. Phys. Chem.* **1966**, *70*, 3437.
(37) Hiemenz, P. C. In *Principles of Colloid and Surface Chemistry*; Marcel Dekker: New York, 1977; Chapter 9.
(38) Ohshima, H.; Healy, T. W.; White, L. R. *J. Colloid Interface Sci.* **1982**, *90*, 17.

(39) Abramowitz, M.; Stegun, I. A. *Handbook of Mathematical Functions*; Dover: New York, 1965.
(40) Feng, X. H.; Dubin, P. L., to be submitted.
(41) Odian, G. *Principles of Polymerization*, 2nd ed.; John Wiley & Sons: New York, 1981.
(42) Morishima, Y., private communication.
(43) Molyneux, P. *Water-Soluble Synthetic Polymers: Properties and Behavior*; CRC Press: Boca Raton, FL, 1984; Vol. 2.

MA010304L